

ARTICLE OPEN



West coast India's rainfall is becoming more convective

A. V. Sreenath¹, S. Abhilash^{1,2}✉, P. Vijaykumar^{1,2} and B. E. Mapes³

A disastrous cloudburst and associated floods in Kerala during the 2019 monsoon season raise the hypothesis that rainfall over the west coast of India, much of which is stratiform, may be trending towards being more convective. As a first exploration, we sought statistically significant differences in monthly ERA-5 reanalysis data for the monsoon season between two epochs, 1980–1999 and 2000–2019. Results suggest a more convective (deeper, ice-rich) cloud population in recent decades, with patterns illustrated in ERA-5 spatial maps. Deepening of convection, above and beyond its trend in amount, is also indicated by the steeper regression slope of outgoing longwave radiation trends against precipitation than that exhibited in interannual variability. Our reanalysis results are strengthened by related trends manifested in more direct observations from satellite and gauge-based rainfall and a CAPE index from balloon soundings data.

npj Climate and Atmospheric Science (2022)5:36; <https://doi.org/10.1038/s41612-022-00258-2>

INTRODUCTION

Model studies predict that the geographic distribution of precipitation will change in response to global warming^{1,2}. In the tropics, these changes have been reflected as 'wet-gets-wetter' (increased rainfall in presently rainy regions)^{3,4} or 'warmer-gets-wetter' (increased rainfall where the rise in sea surface temperature (SST) exceeds the mean surface warming)^{4,5} pattern. Furthermore, mean ocean warming leads to enhancement of extreme precipitation and a decline in light and moderate rainfall^{6,7}, especially in regions where SST warms most. The secular SST warming trend of the Indian Ocean is greater than most of the tropical Pacific and Atlantic, especially since the 1950s⁸. The Arabian Sea has received special attention because its geographical position substantially impacts the densely populated bordering country, India⁹. Accelerated warming of the Arabian Sea since the 1995s is creating significant effects on intense cyclones over the Arabian Peninsula and Indian subcontinent¹⁰. That study also found that warmer winters and decreased decadal rainfall associated with warming of the Arabian sea are accompanied by the decline of wheat production and vegetation cover, respectively.

Studies revealed that there had been a decrease in the probability of moderate rainfall events over central India during the monsoon seasons between the 1951–2000 period, accompanied by enhanced extreme rainfall events⁶. Model projections suggest that the Asian monsoon domain has larger changes in extreme precipitation indices than other monsoon domains¹¹, indicating higher sensitivity of Asian monsoons to global warming. Several hypotheses have been proposed to explain a long-lasting drying trend in Indian Monsoon Summer Rainfall (ISMR). Based on the Community Climate Model Version 3 simulations¹², the first hypothesis attributes the drying trend to the weakening of meridional SST gradient from the equatorial region to the South Asian coast during summer, weakens the monsoon circulation and ultimately results in lower monsoon rainfall over India. Similarly, Roxy et al.¹³ suggested that the warming of the Western Indian Ocean (WIO) has a primary role in the observed decrease of ISMR. An alternative hypothesis suggests that large-scale deforestation may have weakened evapotranspiration and, hence, ISM precipitation over land. Additionally, several studies propose that

higher aerosol emissions in northern India created a cooling effect over the Indian subcontinent, eventually reducing ISMR^{14,15}. Of course, all these effects may occur together.

Greenhouse gas-driven modelling studies suggest that the forced response may be a nearly uniform warming of the tropical Indian Ocean, leading to intensified evaporation, enhanced moisture availability in the atmosphere, and hence increased monsoon rainfall in India^{16,17}. Kitoh et al.¹⁸ noted that despite a modest weakening of the low-level monsoon winds over the Arabian Sea, summer monsoon rainfall over India increased due to enhanced moisture content in the warmer troposphere. On a planetary scale, Wang et al.¹⁹ reported that northern hemisphere summer monsoon rainfall, and the Hadley and Walker circulations, have exhibited substantial intensification during the last three decades (1979–2011), with a striking increase of monsoon rainfall by 9.5% per degree of global warming. Based on observational data sets, Jin et al.²⁰ investigated whether and how the ISMR has increased, specifically in the early part of the 21st century. They find a robust ISMR increase since 2002, closely associated with a favourable land-ocean temperature gradient, driven by a strong warming signature over the Indian subcontinent and slower warming rates over the Indian Ocean. Hari et al.²¹ suggested that this increase of ISMR since 2002 is related to the changes in ITCZ dynamics, which is strengthened and displaced northward as a part of changes in the energy and moisture budgets.

The agrarian-based economy of India crucially depends on the summer monsoon rainfall²², and variation in rainfall has a massive impact on the agricultural output. Both types of extremes (floods and droughts) can adversely affect food security, inflation, and the country's Gross Domestic Product²². Hence, the impact of climate change on the Indian summer monsoon circulation and precipitation pattern is of great practical interest. Global warming is projected to cause an increase in both the mean Indian monsoon rainfall^{23,24} and the frequency of extreme precipitation events^{25,26}.

Romatschke et al.²⁷ identified eight geographical regions with similar convective cloud system characteristics to those over south Asia. They showed that convection over the Arabian Sea is in systems often containing extensive stratiform regions. Orographically influenced large mesoscale convective systems are prolific producers of precipitation in the Bay of Bengal, Arabian Sea, and

¹Department of Atmospheric Sciences, Cochin University of Science and Technology, Cochin 682016, India. ²Advanced Centre for Atmospheric Radar Research, Cochin University of Science and Technology, Cochin 682022, India. ³University of Miami, Miami, FL, USA. ✉email: abhimets@gmail.com

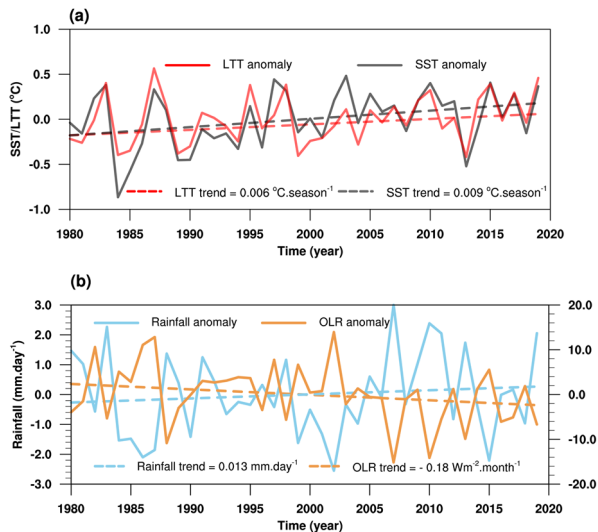


Fig. 1 Interannual variability of LTT, SST, rainfall and OLR. **a** Interannual variability of anomalous sea surface temperature (SST) (°C, black) and lower tropospheric temperature (LTT: 1000 hPa to 700 hPa average) (°C, red) anomalies respectively over the Arabian sea (65–70 °E and 15–20 °N) and the western coast of India (73–77 °E and 8–20 °N) during JJAS. **b** Interannual variability of anomalous rainfall (mm.day⁻¹, Blue) and OLR(Wm⁻², Orange) anomalies, respectively, over the western coast of India (73–77 °E and 8–20 °N) during JJAS. Fitted trends obtained by linear regression on year are indicated by dashed lines.

surrounding areas during the monsoon²⁸. They also observed less frequent occurrences of broad stratiform regions over the eastern coast of the Arabian Sea. Consistently, Hirose et al.²⁹ found that horizontal dimensions of the precipitating systems over the Arabian Sea are smaller than those observed over the Bay of Bengal. When strong, moist lower level westerly wind from the warm Arabian Sea encounters the Western Ghats mountain range, the orographic uplift produces ample amounts of rainfall over the windward side of the west coast³⁰.

The west coast of India is considered highly vulnerable to extreme rainfall events and has witnessed several disasters³¹. Drastic changes in the precipitation pattern over the west coast of India were noted by Lyngwa et al.³² and Meenu et al.³³. Kerala (the southwestern state in India) witnessed extreme rainfall events in August 2018 and 2019^{34–37}. Vijaykumar et al.³⁵ detailed how the rain pattern that caused the 2019 flood may be attributable to the unprecedented warm near-coast SST anomalies and clouds' unusually unstable and convective nature. We enquire whether the rainfall characteristics over this focused region (73–77 °E, 8–20 °N) portray any transformations in the recent past. We show that post-2000, there is an increased frequency of intense precipitation rate and deep convective clouds over the west coast, which may be associated with the rising SST of the eastern-Arabian Sea, existence of greater instability and the intensification and expansion of meridional overturning South Asian monsoon circulation.

RESULTS

Warming Eastern Arabian sea and accelerating rainfall

The Indian Ocean plays a regulatory role in the monsoon through the seasonality of meridional oceanic heat transports, themselves related to the seasonal monsoon winds³⁸. As convenient indices of this highly coupled system, here we considered SST anomalies over the Eastern Arabian Sea (65–70 °E, 5–20 °N) and lower tropospheric temperature (LTT) over the west coast of India (73–77 °E, 8–20 °N) for time series analysis (Fig. 1a). These show an

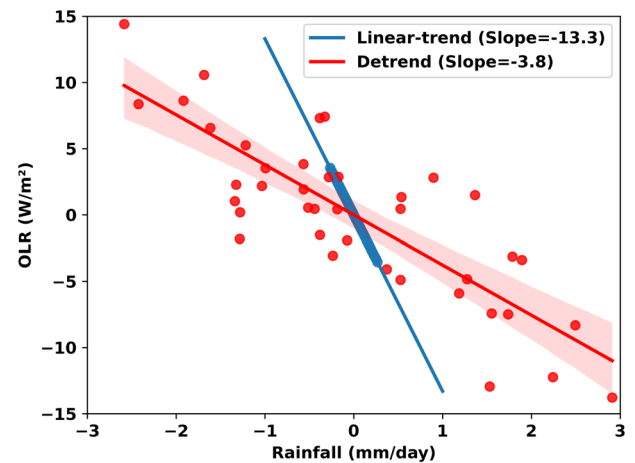


Fig. 2 Trends in rainfall and OLR. Scatter plot between detrend values of rainfall and OLR (red dots) and red shade indicating 95% confidence level. The blue line indicates the linear trend of rainfall and OLR.

in-phase relationship interannually and comparable positive 40-year trends perhaps indicative of forced climate change³⁹, with a robust correlation ($r=0.9$, significant at 95% confidence level). Recently, Jin and Wang (2017)²⁰ reported that there has also been an increase in the land-sea thermal gradient, with more warming inland than the Ocean and subsequently strengthened monsoon over India in post-2002²¹.

Time series of seasonal mean rainfall and outgoing long-wave radiation (OLR) from ERA-5 (see Data and methods) show a rising and falling trend respectively over the west coast (Fig. 1b). These variables are highly anti-correlated on interannual timescales ($r=-0.82$ overall), but the strength of their trends appears to differ distinctly. This is our first hint that cloud tops may be trending upward in altitude, above and beyond the fact that surface precipitation is rising in magnitude. A significant rainfall trend was found by Kumar et al.⁴⁰ in seasonal monsoon rainfall over the west coast. Arun et al.⁴¹ noticed an increasing rainfall in the Konkan and Goa (2.06 mm.year⁻¹) and over the coastal Karnataka (1.79 mm.year⁻¹) along with a non-significant positive trend in peninsular India (0.09 mm.year⁻¹).

Trends in the character of precipitating clouds

Our time series replicates those prior findings of upward rainfall trends (blue curve in Fig. 1b), although this gentle trend is not significant at 95% confidence. We also find a downward trend of OLR (orange curve), which does exceed 95% statistical confidence tests, despite the similar year-to-year noise level in the two-time series. Figure 2 shows scatter and regression results for the data in panel 1b. Precipitation and OLR are highly anti-correlated on interannual timescales ($r=-0.82$, with a best-estimate regression slope of -3.8 Wm^{-2} per mm.day⁻¹ of rain rate). However, the regression of their trends yields a much steeper slope of -13.3 in the same units. This finding suggests that cloud tops may be systematically rising in altitude or expanding in area, above and beyond the secular increase in surface precipitation amount. Either way, it suggests that the character of convective activity is changing as a secular low-frequency trend, not merely the amount. This finding remains somewhat indirect with monthly or seasonal mean reanalysis data as the source. Still, this paper attempts to dig as deeply into aspects of the evidence and validate the sense of the results with more direct (but less complete) observations. Future studies with less-averaged characterisations will be required to fully interpret these results.

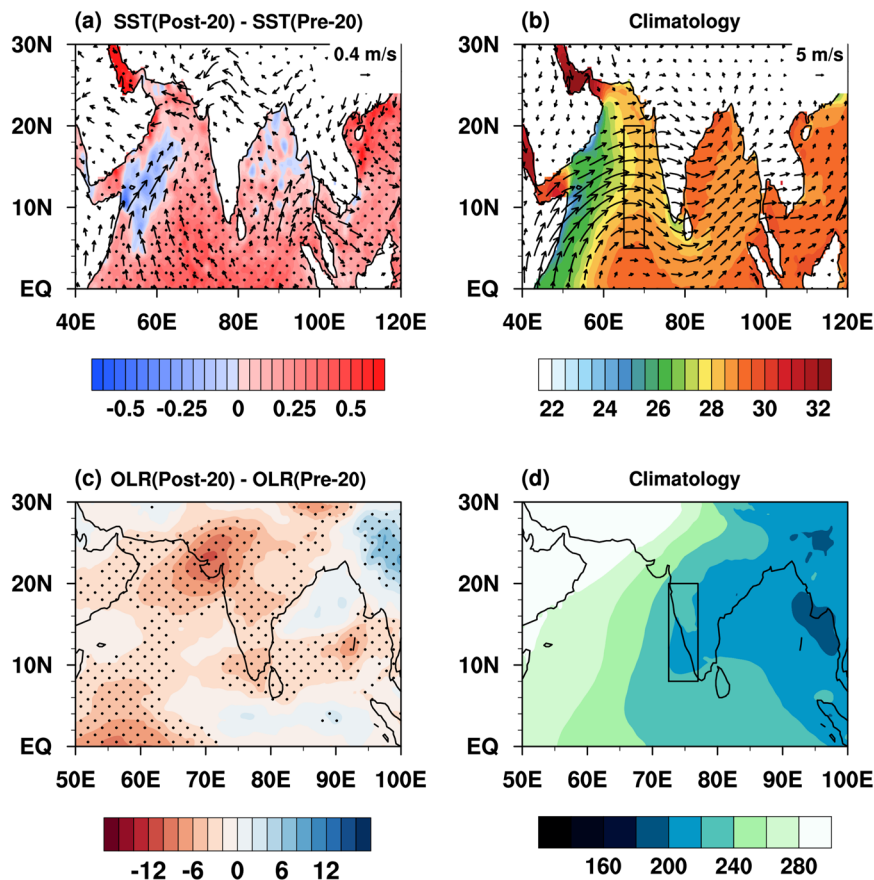


Fig. 3 Changes in SST and OLR. **a** Anomaly (post-20 minus pre-20) JJAS composite SST (unit: °C) with stippling indicates statistically significant areas at a 99% confidence level, overlaid with 850 hPa vector winds (unit: ms^{-1}) significant at a 99% confidence level. **b** SST Climatology. **c**, **d** As above but for OLR (unit: Wm^{-2}). The boxes in **a** and **d** represent the eastern-Arabian sea ($5\text{--}20^\circ\text{N}$, $65\text{--}70^\circ\text{E}$) and west coast of India ($8\text{--}20^\circ\text{N}$, $73\text{--}77^\circ\text{E}$), respectively.

Studies show that the link between SST and convection plays a crucial role in shaping the precipitation over the tropics^{42,43}, but other factors matter too. Besides mean SST warming, SST gradients are also important in determining the tropical circulation and precipitation characteristics⁴⁴. Furthermore, even if the SSTs over a region are conducive for increased convective activity, large-scale circulations could suppress the local convective rainfall⁴⁵. Henceforth, the term “anomaly” or “change” will refer to the difference between post-2000 and pre-2000 composites. Figure 3a indicates that positive SST anomalies (significant at a 99% confidence level) existed over vast areas of the Indian Ocean during post-2000 monsoon seasons, although with negative anomalies over the far western Arabian Sea and spots in the head Bay of Bengal. Because of a shallow mixed layer in summer, SST in the western Arabian Sea is very sensitive to wind-driven upwelling variations^{46,47}, similar to the more famous cold tongue in the equatorial Pacific^{48,49}. Low-level southerly wind anomalies near 10°N display two branches in Fig. 3a: an Arabian Sea branch and a Bay of Bengal branch. The northward wind in the Arabian Sea strengthens where the mean flow (panel b) is directed towards the west coast of India, where its interaction with Western Ghats orography produces copious amounts of rainfall on the west coast of India.

Panel c shows the change of ERA-5 Outgoing Longwave Radiation (OLR). Low values correspond to more cloud amount and/or radiative emission from higher cloud-top altitudes and therefore may be partially a proxy for the top heights of deep clouds^{50,51}. During the post-2000s, extreme negative OLR anomalies are prominent over the north of northwest coast of India. In addition to this, minor but

significant (stippled) minima are spotted over southern peninsular India and the central Bay of Bengal. Might these OLR anomalies during the recent epoch partly reflect the deepening of clouds over the west coast, not merely an increased frequency of occurrence of the same pre-2000 types of clouds?

Intensifying South Asian monsoon circulation

To elucidate the coupling between convection depth and larger-scale South Asian monsoon circulations, consider the vertical-meridional section in the longitude belt $73\text{--}77^\circ\text{E}$ (boxed in Fig. 3d), where the flow is illustrated by arrows in Fig. 4a, b. This monsoon circulation exhibits stronger ascending motion throughout latitudes $>10^\circ\text{N}$ during the post-2000 period (Fig. 4a). In addition, the ascent has become more top-heavy, with the strongest and most significant (stippled) increases above the 500 hPa level, up to 150 hPa in the $15\text{--}20^\circ\text{N}$ latitudes. The corresponding vertical distribution and changes of ERA-5’s specific cloud ice water (SCIW) and specific cloud liquid water (SCLW) over the west coast are depicted in Fig. 4c–f. Climatologically (Fig. 4d), three main ice cores lie between $0\text{--}8^\circ\text{N}$ (1st core), $8\text{--}15^\circ\text{N}$ (2nd core), and $18\text{--}25^\circ\text{N}$ (3rd core).

The climatology of SCLW (panel f) exhibits two well-separated horizontal bands, one in the lower levels (1000–800 hPa) and the other in the middle levels (600–450 hPa) enhanced between 8 and 25°N . These elongated bands are an averaged view of ERA-5’s lower and middle-level clouds over the west coast and suggest characteristic features of the precipitation mechanism. The more flattened nature of the mid-level band may suggest slowly falling recently melted snow and graupel near the 0°C isotherm, while the lower-level condensate may indicate cumulus

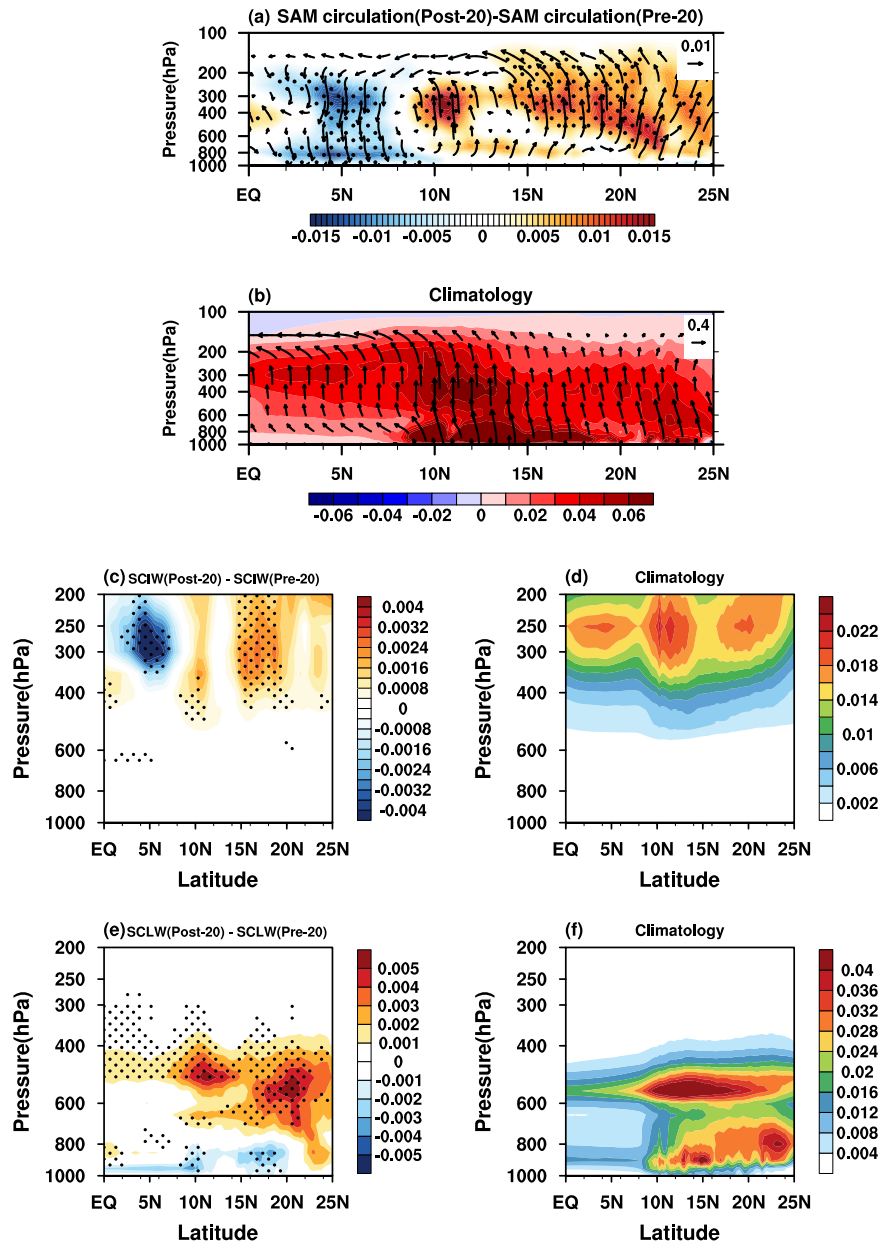


Fig. 4 Changes in SAM circulation and cloud structure. **a** Composite of anomalous negative Omega (shaded) and meridional-vertical wind vectors (units of ms^{-1} for v and -100 Pa s^{-1} for Omega) overlaid with stippling, indicating areas that are statistically significant at a 99% confidence level. **b** Climatology of negative Omega (shaded) and meridional vertical wind vectors. All variables are averaged over $73\text{--}77^\circ\text{E}$. Composite of meridional vertical structures of anomalous (c) SCIW (unit: gkg^{-1}) (e) SCLW (unit: gkg^{-1}) overlaid with stippling indicating statistical significance at a 99% confidence level. Climatology of (d) SCIW and (f) SCLW. SCIW and SCLW are averaged over $73\text{--}77^\circ\text{E}$ in JJAS.

convection near the surface. Statistically significant SCIW changes (Fig. 4c) exhibit two main positive cores: a weak trend over $8\text{--}12^\circ\text{N}$ and a stronger trend over $15\text{--}25^\circ\text{N}$. Both of these are aligned with mid-level SCLW anomalies (panel e), suggestive of anomalies in the melting ice amounts. However, SCLW has significantly decreased near the surface in these same columns, whether by reduced cumulus activity or by scavenging cloud water from SCIW-related precipitation. Whatever the mechanism, the ERA-5 cloud has become more vertically extended, top-heavy and more massive on average.

Checking ERA-5 results against available observations

This section seeks to validate the sense of the ERA-5 results above by using radiosonde, satellite and gauge-based rainfall

observations. Direct observations are valuable, but their space and time coverage is limited, and observing technologies can have spurious drifts, so careful laborious work will be required in the years ahead to confirm these results more fully.

Seeking changes in convective instability, we calculated the twice-daily (at 0000 UTC and 1200 UTC) convective available potential energy (CAPE) by using radiosonde observation downloaded from the University of Wyoming (see Data Sources) for Mangalore (12.9°N , 74.8°E), during 1980–2019 JJAS season. A statistical analysis of these instantaneous CAPE values during the pre-2000 and post-2000 monsoon seasons is shown in box plots (Fig. 5a). The results certainly suggest that CAPE values were significantly higher during the post-2000 epoch (for instance, the median shifted from $\sim 700\text{--}1100 \text{ Jkg}^{-1}$), although the formal

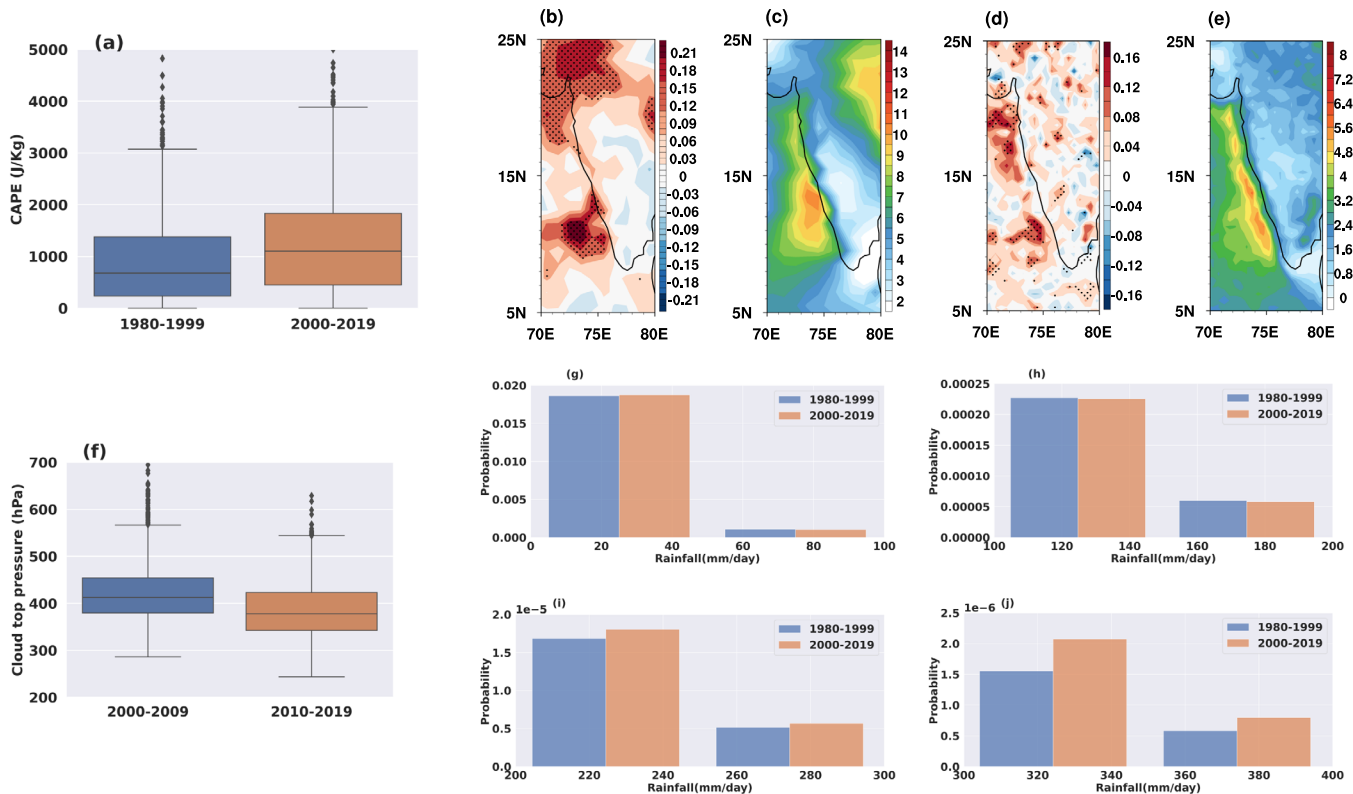


Fig. 5 Trends in CAPE, cloud depth and rainfall from direct observations. **a** Box plot illustrating changes in CAPE during JJAS over the west coast (12.9°N and 74.8°E) from 1980 to 1999 and from 2000 to 2019. In box-part (shaded), the centre line represents the median, bottom and top-line represents the 25th and 75th percentile of data, respectively. The whiskers represent 1.5 times the inner quartile range (IQR), and data outside the 1.5*IQR is identified as outliers. Direct observations of trends by satellite. **b** Spatial patterns of the 1998–2014 linear trends of the average JJAS deep convective cloud cover from ISCCP-H series data (unit: % \cdot day $^{-1}$ 17year $^{-1}$) with stippling indicates statistically significant areas at 95% confidence level. **c** Climatology of deep convective cloud cover (unit: %). **d** Spatial patterns of the 1998–2014 linear trends of the average JJAS convective rainfall from TRMM (unit: mm \cdot day $^{-1}$ 17year $^{-1}$) with stippling indicates statistically significant areas at 95% confidence level. **e** Climatology of convective rainfall (unit: mm \cdot day $^{-1}$). **f** Box plot illustrating the monthly averaged CERES-MODIS cloud top pressure changes during JJAS over the west coast from 2000 to 2009 and from 2010 to 2019. In box-part (shaded), the centre line represents the median, bottom and top-line represents the 25th and 75th percentile of data, respectively. The whiskers represent 1.5 times the inner quartile range (IQR), and data outside the 1.5*IQR is identified as outliers. **g–j** PDF of JJAS rainfall (50 mm \cdot day $^{-1}$ bins between 0 and 400 mm \cdot day $^{-1}$) prepared with the aid of gridded rainfall data from IMD.

significance is not trivial to estimate for this derived variable with its clipped and skewed distribution.

To more directly estimate cloud changes, Fig. 5b–f displays linear trends over the available period of record in cloud cover discriminated by type in ISCCP, cloud top pressure in CERES-MODIS, and a convective rainfall estimate from TRMM (see Data and Methods section). In the climatology of deep convective clouds (Fig. 5c), the distribution varies between 8–16% along the west coast. Trends are all positive over the west coast (warm colours in Fig. 5b). A significant change in deep convective clouds appears from 8°N to 14°N (southern parts of the west coast and offshore), where the background was already fairly large, but a broad area north of about 20°N has also experienced significant (stippled) positive changes.

Convective rainfall from TRMM is more spatially confined than convective cloud, both in its climatology (panel e) and in its trend (panel d), but these changes are in broad agreement with panel b along the coast. Convective clouds have increased more robustly than convective rainfall, another indication of our general hypothesis that the convective process may have deepened, not merely become more frequent. Since satellite precipitation estimates are indirect, gauge-based rainfall are examined in Fig. 5g–j as probability density distributions of daily rainfall in grids obtained from the India Meteorological Department (IMD). Extremely heavy rain events (>244.5 mm \cdot day $^{-1}$)

increased during the recent epoch, consistent with the titular notion and indications above of greater instability and deepening of clouds over the west coast.

In summary, preliminary indications are that summer monsoon clouds systems and precipitation have indeed trended towards more deep-convective characteristics over the west coast of India, as well as increasing in frequency and amount, consistent with changes in the analyzed South Asian monsoon circulation of Fig. 4a during recent decades.

DISCUSSION

In summary, this study inquired whether observed trends in rainfall, rainfall intensity and cloud depth (suggested by downward trends in OLR and upward trends in ice water) may be indicative of an increasingly convective character of rain-making processes over the west coast of India. We further speculated that these may be connected to Arabian Sea warming, greater instability, and strengthened monsoon ascent over western India. If these trends are part of a forced climate signal, they may be likely to continue. Zonal and meridional SST gradients over the Indian Ocean region have also changed, suggesting how nonlocal effects (circulation changes) may also be playing a substantial role, for instance, steering low-level moisture transport towards the west coast. Even larger scales (beyond the basin) also mediate

forced global changes, so more observational and modelling work to answer and extend our title. Internal consistencies among the available data sources examined here bolster confidence in the observed signal, but more big-data work with instantaneous (not seasonally averaged) data is needed to establish and understand the trends. Convection's character is ultimately expressed in the details of thermodynamic profiles, the fine texture of clouds in satellite imagery, and short but impactful extremes in rainfall time series. If trends in these facets of convection continue, ecological and social consequences may be adverse even in places where bulk water resources are and will remain abundant.

METHODS

Reanalysis data

ERA-Interim has been used in many climate studies on clouds in the past^{52–54}. As a successor of ERA-Interim, ERA-5 offers several improvements. Recent studies reported better performance of ERA-5 compared to other reanalysis products in representing various climatic variables, including precipitation, soil moisture, and evaporation, even in the ISMR region⁵⁵. The significant improvements in the horizontal and vertical resolutions of ERA-5 data can result in better estimates of precipitation intensity and orographic precipitation in the western Ghat and foothills of Himalaya⁵⁵. We use monthly averaged ERA-5 data during monsoon season (June to September) from 1980 to 2019 with 0.25° spatial resolution for dynamic (horizontal and vertical wind components), thermodynamic (air temperature, specific humidity), cloud properties (OLR and rainfall) and sea surface temperature. The cloud profile data utilised in this study include specific cloud ice water (SCIW) and specific cloud liquid water (SCLW) with a vertical resolution of 50 hPa. To delineate the changes in circulation and rainfall characteristics during the recent period, we further segregated the years into periods before and after 2000.

Observed data

For the present study, the radiosonde data available at 0000 and 1200 UTC for the 1980–2019 monsoon season at Mangalore station (12.9 °N and 74.8 °E) are used to monitor the thermodynamic state (CAPE) of the atmosphere. For more direct observational confirmation, this study uses 17 years of (1998–2014) of monthly averaged TRMM (Tropical Rainfall Measuring Mission)-3A25v7 data during monsoon season for convective rainfall. The 3A25 product is obtained from the space-time average accumulation of TRMM level-1 and level-2 data (i.e. 1B21, 1C21, 2A21, 2A23, 2A25) on each grid point. The monthly average of convective rain fraction (horizontal resolution: 0.5° (latitude) × 0.5° (longitude)) is obtained by averaging the accumulated passes over each bin for the entire month (For more information: https://www.eorc.jaxa.jp/TRMM/documents/PR_algorithm_product_information/pr_manual/PR_Instruction_Manual_V7_L1.pdf). The ISCCP (International Satellite Cloud Climatology Project) H-series data contain products for monitoring the cloud and surface properties to better understand the effects of clouds on climate, the global hydrologic cycle and the radiation budget. Trends of deep convective cloud cover (10 <= cloud top pressure <= 440hPa, 22.63 < optical thickness <= 450, Cloud top temperature < 253 K) on an equal-area map grid (1° × 1°) were evaluated during the (1998–2014) monsoon season from ISCCP H-series data (Fig. 6a). Cloud top pressure is taken from the CERES-MODIS (Clouds and the Earth's Radiant Energy System-Moderate Resolution Imaging Spectroradiometer) data (1° × 1°) from 2000 to 2019 during JJAS⁵⁶, and a boxplot analysis (Fig. 6e) of cloud top pressure was performed for two decades ((2000–2009) and (2010–2019)) over the west coast. The daily gridded rainfall data from the India Meteorological Department (IMD), available at 0.25° × 0.25° resolution, is prepared using a dense network of rain gauges⁵⁷, are also used to examine the PDF of rain events.

DATA AVAILABILITY

The Era-5, IMD rainfall, radiosonde observation, ISCCP, TRMM and CERES-MODIS data sets can be accessed from the weblinks, <https://www.ecmwf.int/en/forecasts/datasets/reanalysis-datasets/era5>, https://www.imdpune.gov.in/Clim_Pred_LRF_New/Gridded_Data_Download.html, <http://weather.uwyo.edu/upperair/sounding.html>, <https://www.ncei.noaa.gov/products/climate-data-records/cloud-properties-iscsp>, <https://disc.gsfc.nasa.gov/datasets> and <https://ceres.larc.nasa.gov/data/>, respectively.

CODE AVAILABILITY

The computer codes generated during the current study are available from the corresponding author on reasonable request.

Received: 20 June 2021; Accepted: 7 April 2022;

Published online: 12 May 2022

REFERENCES

- Lehmann, J., Coumou, D. & Frieler, K. Increased record-breaking precipitation events under global warming. *Clim. Change* **132**, 501–515 (2015).
- Markus, G., Andrew, L., Lisa, V., Paul, A. & Nicola, M. More extreme precipitation in the world's dry and wet regions, nature climate change. *Nat. Clim. Change* **6**, 508–513 (2016).
- Held, I. M. & Soden, B. J. Robust responses of the hydrological cycle to global warming. *J. Clim.* **19**, 5686–5699 (2006).
- Huang, P., Xie, S.-P., Hu, K., Huang, G. & Huang, R. Patterns of the seasonal response of tropical rainfall to global warming. *Nat. Geosci.* **6**, 357–361 (2013).
- Chadwick, R., Boutle, I. & Martin, G. Spatial patterns of precipitation change in cmip5: Why the rich do not get richer in the tropics. *J. Clim.* **26**, 3803–3822 (2013).
- Goswami, B. N., Venugopal, V., Sengupta, D., Madhusoodanan, M. & Xavier, P. K. Increasing trend of extreme rain events over india in a warming environment. *Science* **314**, 1442–1445 (2006).
- Rajeevan, M., Bhatte, J. & Jaswal, A. K. Analysis of variability and trends of extreme rainfall events over india using 104 years of gridded daily rainfall data. *Geophys. Res. Lett.* **35**, L18707 (2008).
- Han, W. et al. Indian ocean decadal variability: a review. *Bull. Am. Meteorol. Soc.* **95**, 1679–1703 (2014).
- Shukla, J. & Misra, B. M. Relationships between sea surface temperature and wind speed over the central arabian sea, and monsoon rainfall over india. *Mon. Weather. Rev.* **105**, 998–1002 (1977).
- Kumar, S. P., Roshin, R. P., Narvekar, J., Kumar, P. D. & Vivekanandan, E. Response of the arabian sea to global warming and associated regional climate shift. *Mar. Environ. Res.* **68**, 217–222 (2009).
- Kitoh, A. et al. Monsoons in a changing world: a regional perspective in a global context. *J. Geophys. Res. Atmos.* **118**, 3053–3065 (2013).
- Chung, C. E. & Ramanathan, V. Weakening of north indian sst gradients and the monsoon rainfall in india and the sahel. *J. Clim.* **19**, 2036–2045 (2006).
- Roxy, M. K. et al. Drying of indian subcontinent by rapid indian ocean warming and a weakening land-sea thermal gradient. *Nat. Commun.* **6**, 1–10 (2015).
- Bollasina, M. A., Ming, Y. & Ramaswamy, V. Anthropogenic aerosols and the weakening of the south asian summer monsoon. *Science* **334**, 502–505 (2011).
- Ramanathan, V. et al. Atmospheric brown clouds: impacts on south asian climate and hydrological cycle. *Proc. Natl Acad. Sci. USA* **102**, 5326–5333 (2005).
- Meehl, G. & Arblaster, J. Mechanisms for projected future changes in south asian monsoon precipitation. *Clim. Dyn.* **21**, 659–675 (2003).
- Douville, H. et al. Impact of co2 doubling on the asian summer monsoon. *J. Meteorol. Soc. Jpn. Ser. II* **78**, 421–439 (2000).
- Kitoh, A., Yukimoto, S., Noda, A. & Motoi, T. Simulated changes in the asian summer monsoon at times of increased atmospheric co2. *J. Meteorol. Soc. Jpn. Ser. II* **75**, 1019–1031 (1997).
- Wang, B. et al. Northern hemisphere summer monsoon intensified by mega-el niño/southern oscillation and atlantic multidecadal oscillation. *Proc. Natl Acad. Sci. USA* **110**, 5347–5352 (2013).
- Jin, Q. & Wang, C. A revival of indian summer monsoon rainfall since 2002. *Nat. Clim. Change* **7**, 587–594 (2017).
- Hari, V., Villarini, G., Karmakar, S., Wilcox, L. J. & Collins, M. Northward propagation of the intertropical convergence zone and strengthening of indian summer monsoon rainfall. *Geophys. Res. Lett.* **47**, e2020GL089823 (2020).
- Gadgil, S. & Gadgil, S. The indian monsoon, gdp and agriculture. *Econ. Polit. Weekly* **41**, 4887–4895 (2006).
- Loo, Y. Y., Billa, L. & Singh, A. Effect of climate change on seasonal monsoon in asia and its impact on the variability of monsoon rainfall in southeast asia. *Geosci. Front.* **6**, 817–823 (2015).
- Guhathakurta, P., Rajeevan, M., Sikka, D. & Tyagi, A. Observed changes in southwest monsoon rainfall over india during 1901–2011. *Int. J. Climatol.* **35**, 1881–1898 (2015).
- Sharmila, S., Joseph, S., Sahai, A., Abhilash, S. & Chattopadhyay, R. Future projection of indian summer monsoon variability under climate change scenario: an assessment from cmip5 climate models. *Glob. Planet. Change* **124**, 62–78 (2015).
- Giorgi, F. et al. Higher hydroclimatic intensity with global warming. *J. Clim.* **24**, 5309–5324 (2011).

27. Romatschke, U. & Houze, R. A. Characteristics of precipitating convective systems in the south asian monsoon. *J. Hydrometeorology* **12**, 3–26 (2011).
28. Romatschke, U., Medina, S. & Houze, R. A. Regional, seasonal, and diurnal variations of extreme convection in the south asian region. *J. Clim.* **23**, 419–439 (2010).
29. Hirose, M. & Nakamura, K. Spatial and diurnal variation of precipitation systems over asia observed by the trmm precipitation radar. *J. Geophys. Res. Atmos.* **110**, D05106 (2005).
30. Ogura, Y. & Yoshizaki, M. Numerical study of orographic-convective precipitation over the eastern arabian sea and the ghat mountains during the summer monsoon. *J. Atmos. Sci.* **45**, 2097–2122 (1988).
31. Rajan, S., Heller, A. & Ranjan, R. Kerala flood disaster: will migration still act as indemnification. *Econ. Polit. Wkly* **3**, 36 (2018).
32. Lyngwa, R. V. & Nayak, M. A. Atmospheric river linked to extreme rainfall events over kerala in august 2018. *Atmos. Res.* **253**, 105488 (2021).
33. Meenu, S. et al. The physics of extreme rainfall event: An investigation with multisatellite observations and numerical simulations. *J. Atmos. Sol.-Terrestrial Phys.* **204**, 105275 (2020).
34. Athira, U., Abhilash, S. & Ruchith, R. Role of unusual moisture transport across equatorial indian ocean on the extreme rainfall event during kerala flood 2018. *Dyn. Atmos. Ocean.* **95**, 101225 (2021).
35. Vijaykumar, P. et al. Kerala floods in consecutive years-its association with mesoscale cloudburst and structural changes in monsoon clouds over the west coast of india. *Weather. Clim. Extremes* **33**, 100339 (2021).
36. Chaluvadi, R., Varikoden, H., Mujumdar, M., Ingle, S. & Kuttippurath, J. Changes in large-scale circulation over the indo-pacific region and its association with 2018 kerala extreme rainfall event. *Atmos. Res.* **263**, 105809 (2021).
37. Vishnu, C. et al. Satellite-based assessment of the august 2018 flood in parts of kerala, india. *Geomatics Nat. Hazards Risk* **10**, 758–767 (2019).
38. Loschnigg, J. & Webster, P. J. A coupled ocean–atmosphere system of sst modulation for the indian ocean. *J. Clim.* **13**, 3342–3360 (2000).
39. Trenberth, K. E. et al. Observations: surface and atmospheric climate change. *In Climate Change 2007: The Physical Science Basis. Contribution of Working Group 1 to the 4th Assessment Report of the Intergovernmental Panel on Climate Change* (Cambridge University Press, 2007).
40. Kumar, K. R., Pant, G., Parthasarathy, B. & Sontakke, N. Spatial and subseasonal patterns of the long-term trends of indian summer monsoon rainfall. *Int. J. Climatol.* **12**, 257–268 (1992).
41. Mondal, A., Khare, D. & Kundu, S. Spatial and temporal analysis of rainfall and temperature trend of india. *Theor. Appl. Climatol.* **122**, 143–158 (2015).
42. Izumo, T., Vialard, J., Lengaigne, M. & Suresh, I. Relevance of relative sea surface temperature for tropical rainfall interannual variability. *Geophys. Res. Lett.* **47**, e2019GL086182 (2020).
43. Zhang, Y. & Fueglistaler, S. Mechanism for increasing tropical rainfall unevenness with global warming. *Geophys. Res. Lett.* **46**, 14836–14843 (2019).
44. Lindzen, R. S. & Nigam, S. On the role of sea surface temperature gradients in forcing low-level winds and convergence in the tropics. *J. Atmos. Sci.* **44**, 2418–2436 (1987).
45. Lau, K., Wu, H. & Bony, S. The role of large-scale atmospheric circulation in the relationship between tropical convection and sea surface temperature. *J. Clim.* **10**, 381–392 (1997).
46. Montégut, C. B. et al. Simulated seasonal and interannual variability of the mixed layer heat budget in the northern indian ocean. *J. Clim.* **20**, 3249–3268 (2007).
47. Fischer, A. S. et al. Mesoscale eddies, coastal upwelling, and the upper-ocean heat budget in the arabian sea. *Deep. Sea Res. Part II: Top. Stud. Oceanogr.* **49**, 2231–2264 (2002).
48. Zheng, Y., Lin, J.-L. & Shinoda, T. The equatorial pacific cold tongue simulated by ipcc ar4 coupled gcms: Upper ocean heat budget and feedback analysis. *J. Geophys. Res. Oceans* <https://doi.org/10.1029/2011JC007746> (2012).
49. Jiang, W., Huang, P., Li, G. & Huang, G. Emergent constraint on the frequency of central pacific el niño under global warming by the equatorial pacific cold tongue bias in cmip5/6 models. *Geophys. Res. Lett.* **47**, e2020GL089519 (2020).
50. Kidder, S. Q., Kidder, R. M. & Haar, T. H. V. *Satellite Meteorology: An Introduction* (Gulf Professional Publishing, 1995).
51. Gadgil, S., Vinayachandran, P. & Francis, P. Droughts of the indian summer monsoon: role of clouds over the indian ocean. *Curr. Sci.* **85**, 1713–1719 (2003).
52. Jiang, X., Waliser, D. E., Li, J.-L. & Woods, C. Vertical cloud structures of the boreal summer intraseasonal variability based on cloudsat observations and era-interim reanalysis. *Clim. Dyn.* **36**, 2219–2232 (2011).
53. Cuzzone, J. & Vavrus, S. The relationships between arctic sea ice and cloud-related variables in the era-interim reanalysis and ccsm3. *Environ. Res. Lett.* **6**, 014016 (2011).
54. Hanley, J. & Caballero, R. Objective identification and tracking of multicentre cyclones in the era-interim reanalysis dataset. *Q. J. R. Meteorol. Soc.* **138**, 612–625 (2012).
55. Mahto, S. S. & Mishra, V. Does era-5 outperform other reanalysis products for hydrologic applications in india? *J. Geophys. Res. Atmos.* **124**, 9423–9441 (2019).
56. Platnick, S. et al. The modis cloud products: algorithms and examples from terra. *IEEE Trans. Geosci. Remote Sens.* **41**, 459–473 (2003).
57. Pai, D., Rajeevan, M., Sreejith, O., Mukhopadhyay, B. & Satbha, N. Development of a new high spatial resolution (0.25×0.25) long period (1901–2010) daily gridded rainfall data set over india and its comparison with existing data sets over the region. *Mausam* **65**, 1–18 (2014).

ACKNOWLEDGEMENTS

The authors would like to thank ECMWF, the University of Wyoming, NOAA, NASA and IMD for making available the datasets. In addition, Sreenath A V acknowledges the Council of Scientific and Industrial Research (CSIR), India, for providing financial support.

AUTHOR CONTRIBUTIONS

A.S., S.A.V. and M.B.E designed the study. S.A.V. performed the analysis and wrote the paper with feedback from A.S., V.P. and M.B.E.

COMPETING INTERESTS

The authors declare no competing interests.

ADDITIONAL INFORMATION

Correspondence and requests for materials should be addressed to S. Abhilash.

Reprints and permission information is available at <http://www.nature.com/reprints>

Publisher's note Springer Nature remains neutral with regard to jurisdictional claims in published maps and institutional affiliations.



Open Access This article is licensed under a Creative Commons Attribution 4.0 International License, which permits use, sharing, adaptation, distribution and reproduction in any medium or format, as long as you give appropriate credit to the original author(s) and the source, provide a link to the Creative Commons license, and indicate if changes were made. The images or other third party material in this article are included in the article's Creative Commons license, unless indicated otherwise in a credit line to the material. If material is not included in the article's Creative Commons license and your intended use is not permitted by statutory regulation or exceeds the permitted use, you will need to obtain permission directly from the copyright holder. To view a copy of this license, visit <http://creativecommons.org/licenses/by/4.0/>.

© The Author(s) 2022